Ismail *et al.*
Bulletin of the National Research Centre (2022) 46:226
https://doi.org/10.1186/s42269-022-00916-8

Bulletin of the National Research Centre

RESEARCH Open Access

Flux ceramic tiles based on Egyptian trachyte

A. I. M. Ismail[1], M. S. Elmaghraby[2] and B. N. A. Shalaby[1*]

Abstract

Background: The present title is aiming to study the effects of trachyte additions on the sinterability of the ceramic tiles. Four batches were designed with different trachyte/clay ratios from 10 to 40% and 3% of bentonite.

Results: Chemical and phase composition of the raw materials were investigated using XRF and XRD techniques as well as petrographic examination. The prepared batches were fired from 1140 to 1280 °C, their densification parameters and phase compositions as well as microstructure were investigated. Petrographically, the studied trachytic rocks are fine to medium grained, grayish to dark gray, massive rocks, built up, essentially, of alkali feldspars phenocrysts, mainly sanidine and albite, with less frequent pyroxenes and amphiboles, held together in fine to very fine-grained groundmass. The XRD patterns of the fired batches exhibited mullite and quartz as the main mineral phases.

Conclusions: The densification parameters declared that by rising temperature, the bulk density increased in batches of lower trachyte contents and apparent porosity decreased, while in batches of higher trachyte contents exhibited slight increase. It is evident that the main factors controlling the formation present mullite crystallization are: (A) trachyte/clay content which, consequently, affects the Al_2O_3/SiO_2, (B) alkali contents and (C) firing temperature.

Keywords: Ceramic tile, Clay, Trachyte flux, Mineralogy, Microstructure, Densification parameters

Background

Ceramic tiles are products obtained by fast firing of a mixture of quartz, feldspar, kaolin and clay in specific proportions, within a temperature range from 1200 to 1300 °C. They are characterized by low porosity, good bending strength and hardness as well as wear resistance. Quartz acts as a filler material and forms the skeleton of the ceramic body. Clay and kaolin provide plasticity to the body for shaping and acts as a binding agent to give strength in the state before firing process. Feldspars are used as fluxing agents to lower the sintering temperature during firing by forming a glassy phase. Ceramic bodies are manufactured using large amount (40–50 wt %) of fluxes, such as sodic and potassic feldspars, trachytes, nepheline syenite, talc and glasses as well as raw materials rich in sodium and potassium oxides. From the economic point of view, utilization of cheap raw materials able to replace the traditional fluxes without altering the ceramic quality is of specific importance to reduce the product cost Kayacı (2020), Sanchez (2003), Manfredini et al (1995) and Espasito et al (2005).

Feldspar minerals form vast ratio of mineral groups found in the earth (about 60-65%). They can be classified into two groups: potash feldspars, such as orthoclase, microcline, sanidine and adularia are crystallized in monoclinic system, and anorthoclase has triclinic symmetry, in addition to the plagioclase series, from sodium rich albite to calcium rich anorthite. The group of feldspar minerals which include albite and anorthite have a melting point between 1122 and 1550 °C, while those being of a continuous series of mixed crystals (plagioclase) have a melting point at 1450 °C. Andesine (Ab50-An50) starts to melt at 1287 °C, while orthoclase starts to melt at 1150 °C Kara et al (2006), Sanchez et al (2019), Jones

*Correspondence: baselshalaby@gmail.com

[1] Geological Sciences Department, National Research Centre, Dokki, Cairo, Egypt
Full list of author information is available at the end of the article

and Berard (1972), Klein (2001), Njoyaa et al (2017) and Dondi (1994).

The technological role of fluxes in ceramic bodies focused on liquid phase formation during firing by melting alkali feldspars, sericite and further minerals. Such a liquid phase fills the original porosity of bodies and promotes densification by viscous flow. Finally, the liquid turns into a vitreous phase during cooling. So, the chemical composition of fluxes reflects their technological behavior and effects during sintering of the ceramic bodies. Batches with very high fusibility are expected by quartz-free and feldspathoid-bearing fluxes like nepheline syenites and phonolites. Batches show high fusibility is characteristic of quartz-poor and sodium-rich feldspar as in albitites and some pegmatitesas well asaplites; medium-to-low fusibility is found for quartz-poor fluxes and mixed Na-K feldspars or sericite, as most pegmatites, aplites, phyllites and some granitoids. Low-to-very low fusibility is observed when fluxes have large amount of quartz and mixed feldspars, especially with a potassic content, like in granitoids, acid volcanics and arenites. Compared to feldspathic fluxes, waste glasses usually have a low percentage of alumina and a high amount of alkaline and alkaline earth oxides. In addition, some types contain elements—like barium, strontium and boron—that in primary fluxes are present just in traces. Such chemical features lead to these secondary fluxes an extremely high fusibility, with softening and melting temperatures comparable to basalts Dondi (2018a; b), Bozzola et al (2012), Brown and Mackenzie (1992), Brown et al (2016a, b), Brown et al (2016a, b), Dondi et al (2001), Dondi et al (2014), and Dondi (2018a; b).

Geologically, during Phanerozoic and after ceasing of the Pan African orogeny (650-550 Ma), seven cycles of interplate magmatism were encountered in the Eastern Desert of Egypt, extended from Paleozoic to Cenozoic Eras (600-30 Ma), the Paleozoic magmatism comprises Late Carboniferous, Permian, and Permo-Triassic magmatism, the Mesozoic magmatism encountered early Triassic, late Jurassic, early and late cretaceous magmatisms, the Cenozoic magmatism represented by Tertiary and Oligocene—Miocene magmatism. These volcanic activities resulted in formation of different types of magma series ranged from transitional to alkaline—peralkaline magma series. The main crystallized rock units are alkali basalts, trachytes, phonolites and alkaline to peralkaline rhyolites, with their plutonic equivalents, existing in the form of volcanic plugs, intrusions, ring complexes, sills and dykes. The composition of their parental magma varies from silica under-saturation (nepheline normative) to silica-saturated (olivine normative) to silica over-saturation (quartz normative). Tectonically, these rocks are thought to be evolved on an orogemic tectonic regime (Stern (1981), Harris (1982), Hashad (1994), Abdel-Rahman (1995), Aly and Shalaby (2001), Mohamed (2001), Gharib and Obeid (2012) and Shalaby et al (2017), (2018), (2019)).

Methods

The aim of the present work is to study the effect of trachyte additives as a flux on the ceramic production. To achieve this purpose, four batches of trachyte/clay ratios were designed as 10/90, 20/80, 30/70 and 40/60% in order to evaluate the fluxing effect of the trachyte rock on the sinterability of the batches.

The materials used to achieve the above-mentioned objective are trachyte, Aswan clay and bentonitic clay. Trachyte rocks were collected from Gabal Umm Shaghir, located to the southwest of Qusseir city Red Sea coast, Egypt, at Lat. 25° 58′ 17″ N and Longi. 33° 54′ 04″ E. It is highly elevated, cone-like hill, built up of massive, hard, buff to pinkish gray trachytic rocks. It is considered to be the youngest rock unit of the mapped area, Fig. 1, as it intrudes, the surrounding Precambrian country rocks, represented mainly by Metasediments, Metavolcanics, Serpentinites, Older granite, Dokhan Volcanics and Younger granites. Aswan clay was received from Normatic Co. for building materials and refractories, Helwan, Cairo, Egypt, while bentonite was derived from Alexandria Company.

The prepared raw materials, used in this study, composed of Aswan clay, Umm Shaghir trachyte and 3% bentonite to increase the plasticity and the green strength. The materials were crushed, ground and passed through 63-micron sieve. The mineral composition of the starting materials was studied using XRD and petrographic study of the thin section for the trachytic rocks. The chemical composition was investigated using XRF technique for the trachyte, clay and bentonitic clay. Plasticity of the clay used in this study was also practiced to evaluate the liquid limit and plasticity. The phase composition of the fired products was studied using XRD technique to estimate the new phases formed after firing. Densification parameters of the fired products as well as the microstructure and microchemistry of some selected samples were also performed.

The XRD analysis was performed using a Philips X-ray Diffraction equipment model X′ Pert PRO with Monochromator, Cu-radiation (1.542 Å) at 50 K.V., 40 M.A. and scanning speed 0.02°/sec. The XRF analysis was carried out for powder (< 74 μm) samples using X-ray fluorescence equipment PW 2404 with six analyzing crystals. The concentration of the analyzed elements is determined by using software SuperQ and SemiQ programs with accuracy 99.99% and confidence limit 96.7%. The estimation of the major oxides was

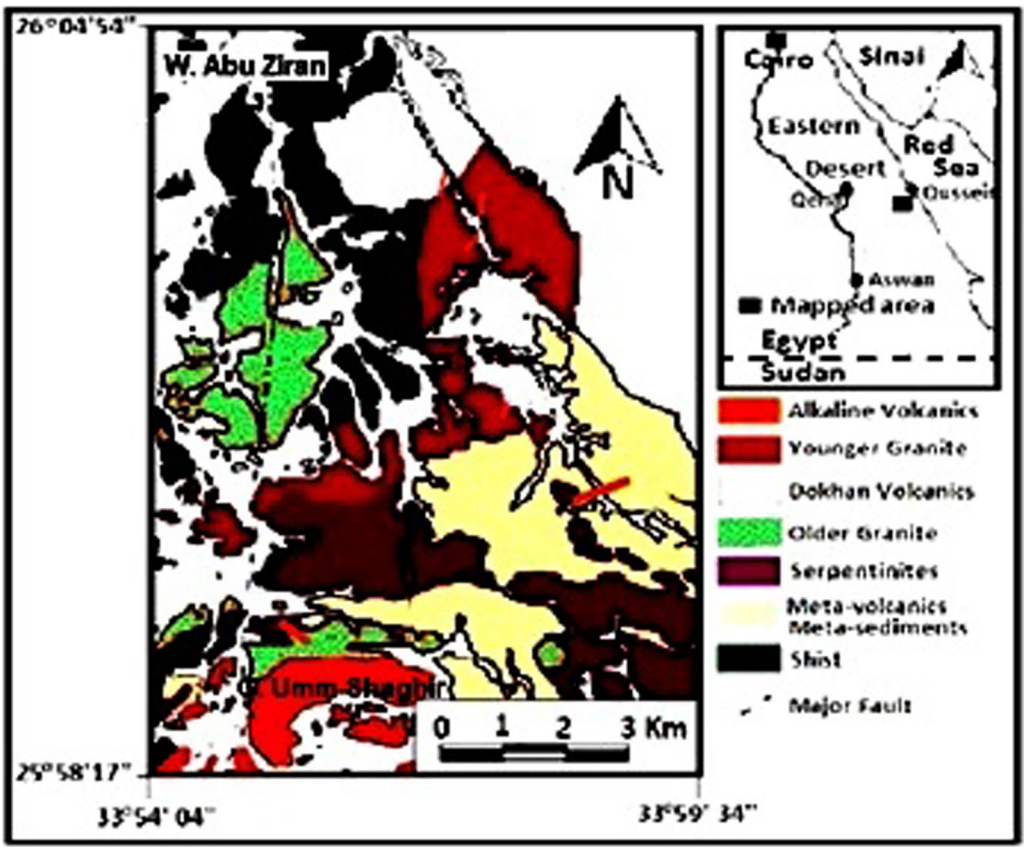

Fig. 1 Geological map of Umm Shaghir Area, (after Shalaby et al. (2019))

done as powder pellets (Pellets method) which were prepared by pressing the powder of the sample in Aluminum Cup using Herzog presser and 10-ton pressure. A scanning electron microscope (SEM) has been used in this study for both microstructure and mineralogical identification. Microchemistry using the scanning electron microscope attached with EDAX unit was carried out for some selected batches. The scanning electron microscope using SEM Model Quanta 250 FEG (Field Emission Gun) attached with EDAX Unit (energy dispersive X-ray analyses), with accelerating voltage 30 K.V. and magnification14× up to 1,000,000.

The chemical composition of the raw materials is summarized in Table 1. Simulation of the industrial processing was done on laboratory scale, by milling in dry condition (15 min in planetary mill with porcelain jar and porcelain grinding media). 3% of bentonite was added to increase the plasticity of the batches. Powders were shaped into 30 × 30 × 5 mm tiles by hydraulic pressing (35 MPa) and then dried in oven (110 °C overnight) and fast fired in an electric furnace (temperature from 1140 to 1280 °C; 30 minutes soaking time).

Table 1 Chemical composition of the used raw materials

Oxides %	Trachyte	Clay	Bentonite
SiO_2	61.81	52.97	53.12
Al_2O_3	16.69	29.07	15.98
TiO_2	0.18	1.48	1.15
Fe_2O_3	4.95	3.92	9.24
CaO	1.12	0.5	0.81
MgO	0.29	0.2	3.77
Na_2O	7.97	0.06	4.26
K_2O	4.37	0.28	0.83
SO_3	0.06	0.76	0.76
ZrO2	0.25	–	–
Cl	–	–	1.45
LOI	1.62	10.62	8.15
Total	99.31	99.86	99.52

Some technological behaviors of the samples were determined in dry state and after firing up to 1280 °C; for 30 min. Linear shrinkage and bulk density were determined for dry samples and fired tiles; in addition to water

absorption, apparent porosity was determined for fired tiles. Sintering curves versus the firing temperature were drawn using linear shrinkage, water absorption, porosity and bulk density. Phase composition and microstructure of some selected fired batches were investigated using XRD and SEM as well as EDAX, respectively.

The methods of the present study were done according to the regulations of the National Research Centre. The present research works were done on teste items, as natural stones and minerals, so, it is unnecessary to approve this research work according to national regulations of institutional ethics committee.

Results

Petrographically, the studied trachytic rocks are fine to medium grained, grayish to dark gray, massive rocks, built up, essentially, of alkali feldspars phenocrysts, mainly sanidine and albite, with less frequent pyroxenes and amphiboles, held together in fine to very fine-grained groundmass. The sanidine phenocrysts reach in size up 3 mm in length and 1 mm in breadth, and they are simply twinned, euherdral to subhedral crystals, usually exhibiting various degrees of alteration to kaoline and sericite (Fig. 2). The albite phenocrysts are found in the form of prismatic crystals their dimensions reach up to 5 mm in length and 2 mm in breadth, and they are severely kaolinized and sericitized, and sometimes cracked, tilted and curved due to local stresses resulted from the flowage of the magma (Fig. 3). Primary quartz is rarely observed filing the interspaces between feldspar crystals. The overall felsic content represents more than 90% of the rock volume. The mafic constituents are represented mainly by aegerine, aegerineaugite, with less frequent amounts sodic amphiboles, mainly arvedsonite, sometimes altered to chlorite. The mafic content represents up to 10% of the total rock volume and is usually exist as micro-phenocrysts exist between the interlocked feldspar crystals, and sometimes the mafic crystals intrude the feldspar

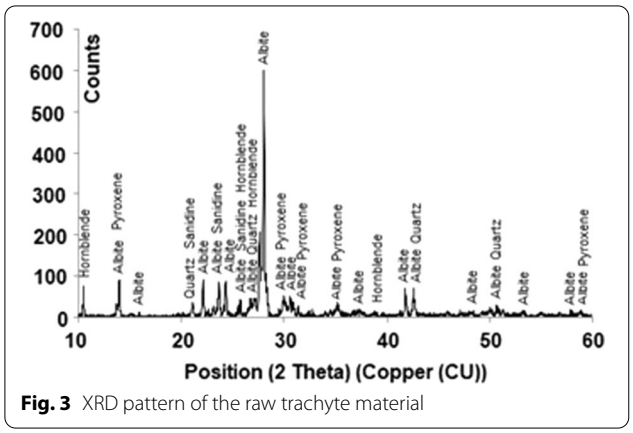

Fig. 3 XRD pattern of the raw trachyte material

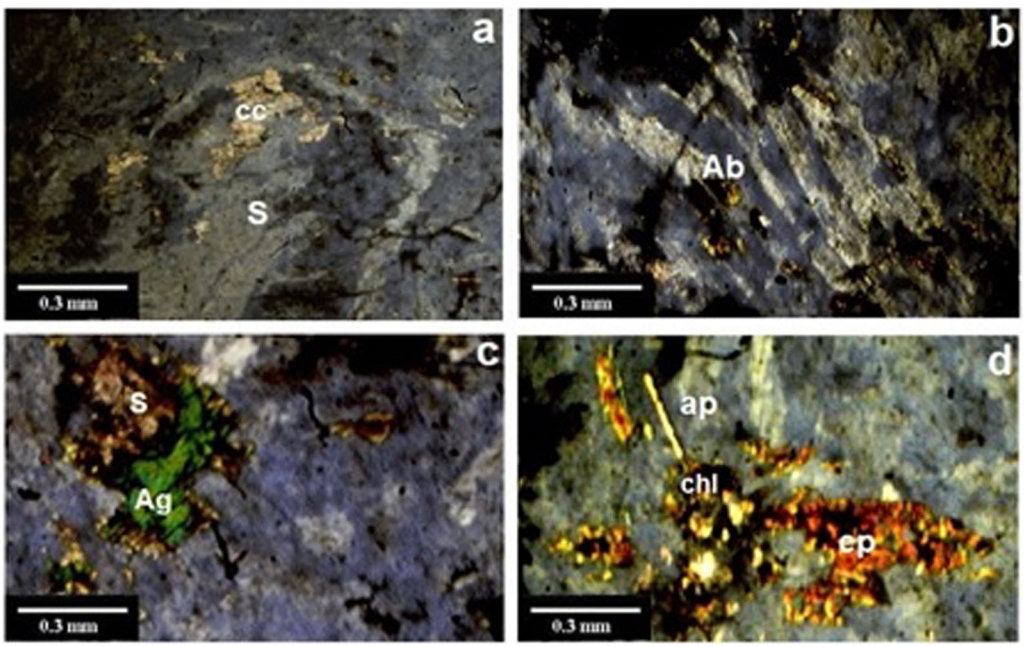

Fig. 2 **a** Photomicrograph showing sanidine crystal (S) phenocryst altered to calcite (cc). (XPL). **b** Photomicrograph showing cracked albitephenocryst (Ab) exhibiting minor displacement along minor fault. (XPL). **c** Photomicrograph showing aegerine (Ag) crystal intruding severely altered sandine crystal (S) in ophetic relation (XPL) **d** Photomicrograph showing epidote (ep), apatite (ap) and chlorite (chl) overgrown on feldspar crystal. (XPL)

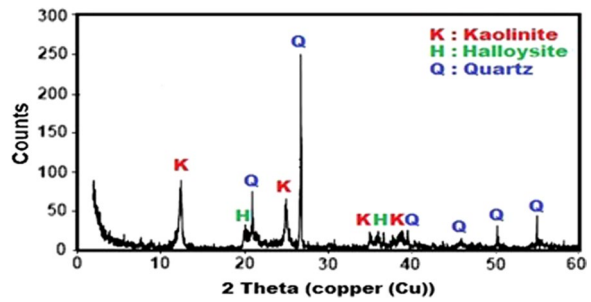

Fig. 4 XRD pattern of the raw clay materials (after El-Maghraby et al. 2019)

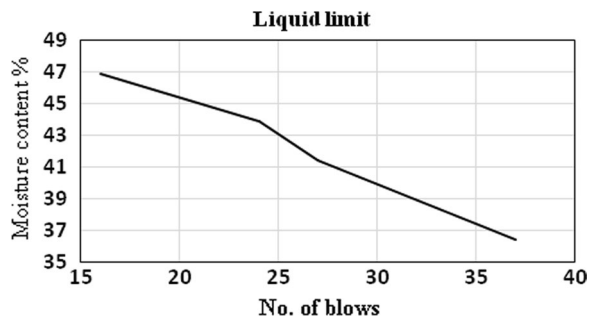

Fig. 5 Water content and liquid of the clay sample**.** Liquid limit (water content at 25 blows) = 43%. Plasticity = liquid limit-plastic limit [43.00—22.00 = 21]

crystals giving rise to ophitic and subophitic textures (Fig. 4). The groundmass is usually cryptocrystalline to microcrystalline feldspar crystals, arranged in preferred orientation giving rise to directive or trachytic textures. The flowed groundmass is usually, attacking and corroding the preexisting feldspars phenocrysts. The main encountered accessory minerals are epidote, apatite, zircon, allanite and iron oxides (Fig. 5).

The XRD pattern of the raw trachyte material confirms that the main mineral phases are albite, sanidine, hornblende and pyroxene with minor quartz, which matches with the petrographic study carried out by the transmitted light polarized microscope. The high intensities of sanidine and albite reflect the alkaline nature of the rock (Fig. 6a). The interstitial beaks of albite and sanidine confirm their co-crystallization. Figure 6b shows the mineralogical composition used clay, and it composed mainly of kaolinite and halloysite as clay minerals in addition to quartz as a non-clay mineral. The chemical composition of the used raw materials is shown in Table 1. The major chemical composition of trachyte is silica (61.81%), alumina (16.69%), Na_2O (7.97%), Fe_2O_3 (4.95%) and K_2O (4.37%), in addition to lesser amounts of CaO (1.12%), TiO_2 (0.18%) and MgO (0.29%).

The chemical composition of the used clay is mainly of silica, alumina, ferric oxides and titania as 52.97, 29.07, 3.92 and 1.48%, respectively. The minor oxides are calcium, magnesium, sodium and potassium. The chemical composition of the bentonitic clay (added for about 3% in all batches) is mainly of silica, alumina, ferric oxide,

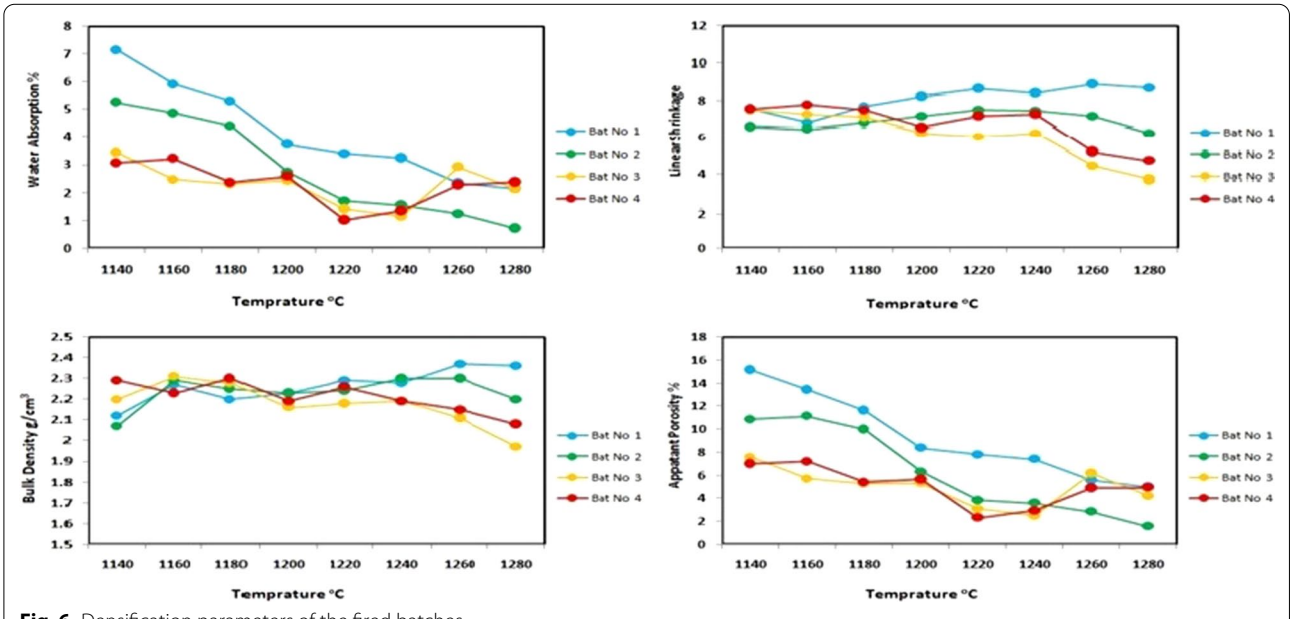

Fig. 6 Densification parameters of the fired batches

Table 2 Chemical composition of the design batch no. 1

Oxides %	10% trachyte	90% clay	Total
SiO_2	6.18	47.67	53.85
Al_2O_3	1.67	26.16	27.83
TiO_2	0.02	1.33	1.35
Fe_2O_3	0.50	3.53	4.03
CaO	0.11	0.45	0.56
MgO	0.03	0.18	0.21
Na_2O	0.80	0.05	0.85
K_2O	0.44	0.25	0.69
SO_3	0.01	0.68	0.69
ZrO2	0.03	–	0.03
LOI	0.16	9.56	9.72
Total	9.95	89.86	99.81

Table 3 Chemical composition of the design batch no. 2

Oxides %	20% trachyte	80% clay	Total
SiO_2	12.36	42.38	54.74
Al_2O_3	3.34	23.26	26.60
TiO_2	0.04	1.18	1.22
Fe_2O_3	0.10	3.14	3.24
CaO	0.22	0.4	0.62
MgO	0.06	0.16	0.22
Na_2O	1.60	0.05	1.65
K_2O	0.87	0.22	1.09
SO_3	0.01	0.61	0.62
ZrO2	0.05	–	0.05
LOI	0.32	8.50	8.82
Total	18.97	79.90	98.87

Table 4 Chemical composition of the design batch no. 3

Oxides %	30% trachyte	70% clay	Total
SiO_2	18.54	37.08	55.62
Al_2O_3	5.01	20.35	25.36
TiO_2	0.05	1.04	1.09
Fe_2O_3	1.49	2.74	4.23
CaO	0.34	0.35	0.69
MgO	0.09	0.14	0.23
Na_2O	2.39	0.04	2.43
K_2O	1.31	0.20	1.51
SO_3	0.02	0.53	0.55
ZrO2	0.08	–	0.08
LOI	0.49	7.43	7.92
Total	29.81	69.9	99.71

Table 5 Chemical composition of the design batch no. 4

Oxides %	40% trachyte	60% clay	Total
SiO_2	24.72	31.78	56.50
Al_2O_3	6.68	17.44	24.12
TiO_2	0.07	0.89	0.96
Fe_2O_3	1.98	2.35	4.33
CaO	0.45	0.30	0.75
MgO	0.12	0.12	0.24
Na_2O	3.19	0.04	3.23
K_2O	1.75	0.17	1.92
SO_3	0.02	0.46	0.46
ZrO2	0.1	–	0.10
LOI	0.65	6.37	7.02
Total	39.73	59.92	99.63

sodium oxide and magnesia as the main oxides, while the loss on ignition is 8.15% (Table 1).

Four batches, based on trachyte/clay ratios, were designed as 10/90%, 20/80%, 30/70% and 40/60%, respectively, and the chemical composition of the four designed batches are given in Tables 2, 3, 4 and 5. It is noticed that by increasing the trachyte/clay ratio, the silica and iron oxide contents slightly increase from 53.85 to 56.50% and 4.03 to 4.33%, respectively, alkalis (Na_2O+K_2O), also increase from 1.54% in batch no. 1 to 5.15% in batch no. 4, while Al_2O_3 decreases from 27.83% in batch 1 to 24.12% in batch 4.

The determined plastic and the liquid limits (BS 1377 1975) of the used clay material are 22% and 43%, respectively, while the plasticity is 21 (Fig. 5). The amount of water that rendered the raw clay material plastic (i.e., plasticity) was determined using the Atterberg method (BS 1377 1975) (28-29). It is also noticed that there is no remarkable change in the shrinkage or expansion of the green batches after drying at 105 °C, as shown in Table 6.

Table 6 Linear shrinkage of the green batches after drying at 105 °C

Batch no	1	2	3	4
Before drying	30.29	30.71	30.67	30.67
After drying	30.29	30.70	30.62	30.67

Discussion

The relation between bulk density and the firing temperature in the fired four batches declared that batch no. 1 shows slight increase in the bulk density by increasing the firing temperature, while batches nos. 2–4 exhibit irregular behavior by increasing the temperature; the lowest

densities are recorded at 1280 °C for batches nos. 3 and 4, (1.97 and 2.08 g/cm^3, respectively), while the maximum bulk densities are 2.31, 2.30, 2.30 and 2.36 g/cm^3, for batches nos. 3, 4, 2 and 1 at temperatures of 1160, 1180, 1260 and 1280 °C, respectively. It is also noticed that by increasing the temperature, the bulk density increases in the batches of lower trachyte contents, while those of higher trachyte contents exhibit lower densities with increasing firing temperature (Table 7 and Fig. 6).

The apparent porosity and water absorption values decrease, as the firing temperature rises; however, in bathes nos. 3 and 4, the apparent porosity and water absorption decrease till 1240 °C and 1220 °C, respectively, and start to increase again till 1280 °C. The increase in the apparent porosity and water absorption in such temperature ranges is due to the bloating and seepage of the high content of the liquid phase and formation of new pores.

The shrinkage in batch no. 1 increases with an increase in the temperature, while in the other three batches, the shrinkage decreases, slightly, till 1280 °C.

The XRD patterns of the fired four batches at 1160 °C, 1180 °C, 1240 °C and 1280 °C, exhibited formation of mullite and quartz as the main mineral phases recorded in the all fired batches, in addition to less frequent cristobalite crystals. The highly crystalline mullite and quartz phases were formed in batch no. 1, fired at 1280 °C, while

Table 7 Densification parameters of the fired batches

Firing temperature °C	Batch no	Bulk density (g/cm^3)	Apparent porosity (%)	Water absorption (%)	Linear shrinkage
1140	1	2.12	15.15	7.15	7.53
	2	2.07	10.86	5.25	6.60
	3	2.20	7.58	3.45	7.51
	4	2.29	7.0	3.06	7.56
1160	1	2.27	13.43	5.92	6.80
	2	2.29	11.14	4.86	6.48
	3	2.31	5.71	2.47	7.25
	4	2.23	7.19	3.22	7.79
1180	1	2.20	11.63	5.29	7.68
	2	2.25	10.0	4.40	6.79
	3	2.28	5.28	2.32	7.11
	4	2.30	5.42	2.36	7.48
1200	1	2.23	8.37	3.75	8.24
	2	2.23	6.29	2.73	7.13
	3	2.16	5.30	2.45	6.24
	4	2.19	5.66	2.59	6.55
1220	1	2.29	7.79	3.40	8.65
	2	2.24	3.83	1.71	7.49
	3	2.18	3.10	1.42	6.04
	4	2.26	2.31	1.02	7.17
1240	1	2.28	7.40	3.25	8.42
	2	2.30	3.58	1.56	7.43
	3	2.19	2.49	1.14	6.24
	4	2.19	2.95	1.35	7.27
1260	1	2.37	5.58	2.35	8.91
	2	2.30	2.84	1.24	7.14
	3	2.11	6.17	2.92	4.44
	4	2.15	4.90	2.28	5.22
1280	1	2.36	5.0	2.15	8.68
	2	2.20	1.56	0.72	6.25
	3	1.97	4.21	2.14	3.72
	4	2.08	4.93	2.38	4.73

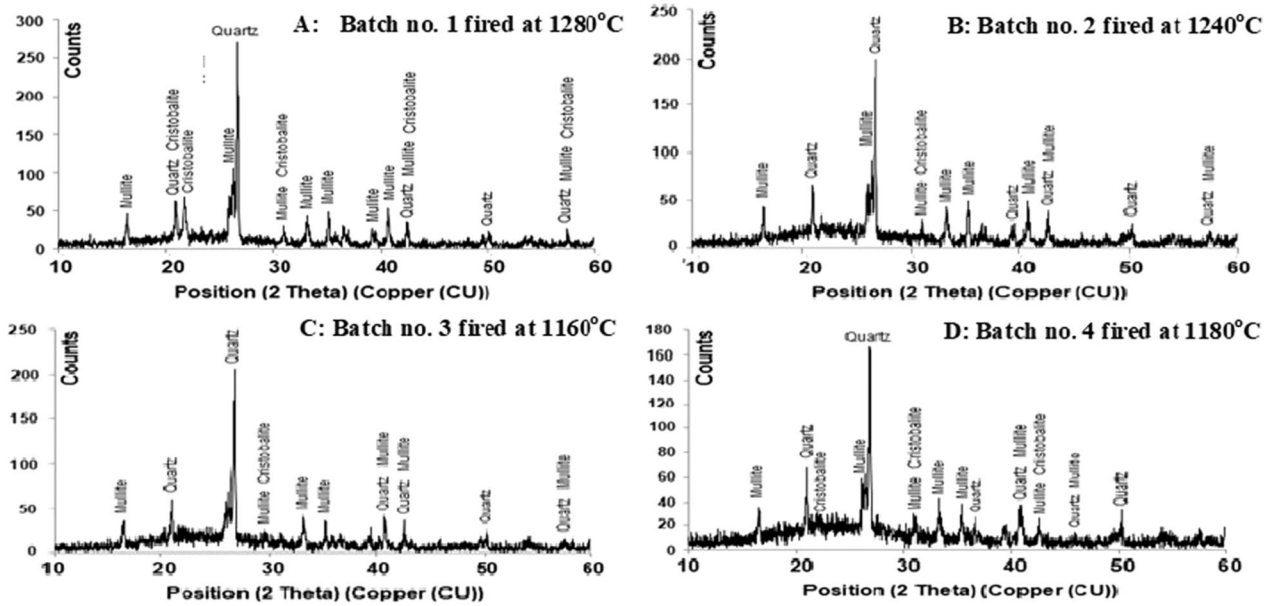

Fig. 7 XRD patterns of the fired batches

the least crystalline phases are recorded in batch no. 4 fired at 1180 °C, Fig. 7.

The SEM and EDAX of some selected batches fired at 1160, 1200, 1240 and 1280 °C, confirmed that mullite is the sole crystalline phase, usually has subhedral forms, embedded in glassy phase groundmass. In case of batches fired at 1160 °C, Fig. 8a, b and c, the liquid phase exists in relatively restricted amounts, and as the firing temperature raises, the liquid phase contents increase and larger mullite crystals are well-developed (Fig. 8d, e and f). It is also noticed that by increasing trachyte additives, the batch becomes more enriched by alkali oxides, which leads to increase in the liquid amount. On the other hand, as the firing temperature rises, the liquid phase content increases giving rise to convenient conditions for the mullite crystals to develop in larger sizes within the surrounding glassy matrix (Fig. 8g, h, I and k). The most developed mullite crystals are detected in batches nos.1 and 2, fired at 1160 °C, with the mixtures of highest clay contents, (i.e., highest alumina content) and lower trachyte content, (i.e., lower silica and alkali contents) ratios (Fig. 8k and l).

The EDAX analysis shows that crystal composition at point (a) is mainly aluminum silicate referring to the mullite mineral, while the glassy phase composition at points (b and c) is mainly alkali silicates such as sodium, potassium, in addition to magnesium, and aluminum silicate.

From the previously mentioned results, it is evident that the main factors controlling the present mullite crystallization are: (1) Al_2O_3/SiO_2, which is related to the trachyte/clay ratios, (2) the alkalis contents and (3) the firing temperature.

Conclusions

- The aim of the present work is to study the effect of trachyte additives as a flux on the ceramic sinterability.
- The materials used in this study are clay, trachyte and bentonite.
- The phase composition and plasticity of the clay was studied. The main phase compositions are kaolinite, halloysite and quartz, while plasticity and liquid limit are 21 and 43%, respectively.
- The phase composition and petrographic investigations of the used trachyte revealed that its mineralogical composition is mainly albite and sanidine, with less frequent amounts of pyroxene and amphiboles as mafic constituents, and few quartz crystals are also recorded.
- Four batches of trachyte/clay ratio were designed with 10/90, 20/80, 30/70 and 40/60% and fired from 1140 to 1280 °C.
- The phase composition of the fired batches refers that mullite and quartz are the main phases formed during different fired temperatures and trachyte contents.
- The crystallinity of mullite and quartz increase as a result of less flux content and temperature which dissociate the crystalline phases to the glassy phase.

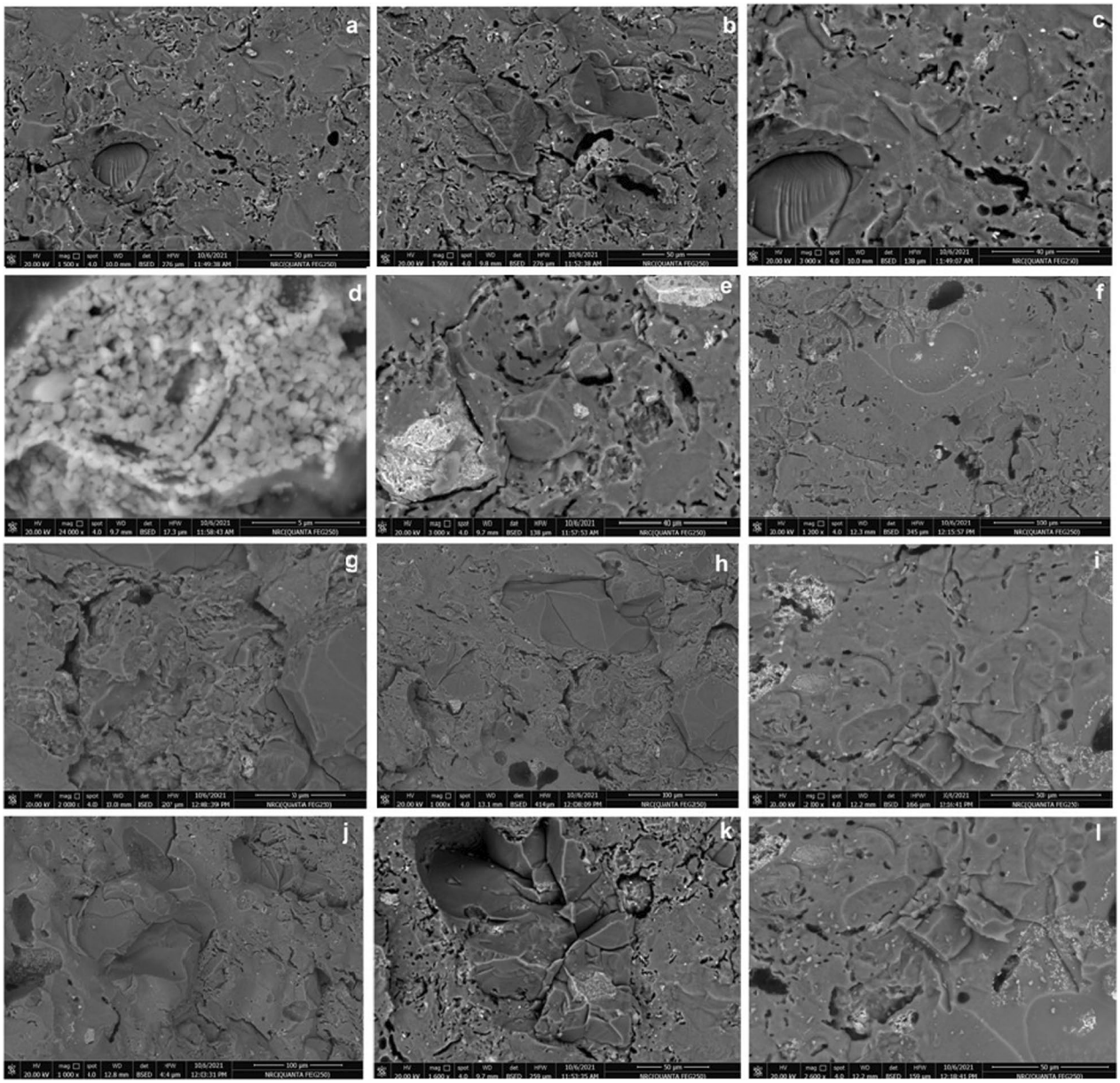

Fig. 8 SEM of the selected fired batches

- Microstructure and microchemistry of selected fired batches using SEM and EDAX confirm existence of mullite phenocrysts embedded in glassy groundmass.
- Densification parameters of the fired batches exhibit that by increasing temperature, the bulk density increases in the batches of lower trachyte contents, while those of higher trachyte contents exhibit lower densities with the increase in temperatures.
- In lower ratios of trachyte contents and at higher firing temperatures, the crystallinity of mullite and quartz increases due to less flux content, which leads to less dissociation of the early developed crystalline phases.

Abbreviations

EDAX: Energy dispersive X-ray analysis; SEM: Scanning electron microscope; XRD: X-ray diffraction; XRF: X-ray fluorescence.

Acknowledgements
The authors are deeply grateful to Geo-mechanical Consultant Unit and Marble and Granite Testing Laboratory Unit, National Research Centre, Egypt, for their continuous support during the preparation of the present article.

Author contributions
AIMI studied the mineralogy, geochemistry and tested physical parameters and interpreted the application works. MSE performed the refractory applications and the preparation of paste samples. BNAS performed the petrographical studies, geochemistry, physical parameters and application works. All authors have read and approved the final manuscript.

Funding
Marble and Granite Lab. Unit and Geo-mechanical Consulting Unit National Research Centre, Cairo, Egypt.

Availability of data and material
Authors declare that the work data and materials are available.

Declarations

Ethics approval and consent to participate
Authors declare that the work is ethically approved and consent to participate. The present research works were done at National Research Centre, and it is unnecessary to approve this research work according to the national regulations of institutional ethics committee.

Consent for publication
Not applicable.

Competing interests
Authors declare that the work has no competing interests.

Author details
[1]Geological Sciences Department, National Research Centre, Dokki, Cairo, Egypt. [2]Ceramics, Refractories and Building Materials Department, National Research Centre, Dokki, Cairo, Egypt.

Received: 8 May 2022 Accepted: 27 June 2022
Published online: 30 July 2022

References

Abdel-Rahman AM (1995) Tectonic–magmatic stages of shield evolution: the Pan-African belt in northeastern Egypt. Tectono-Physics 242:223–240
Aly MH, Shalaby BN (2001) Geochemical characterization of trachytic rocks for stoneware recipes: an example on Abu Khruq trachytic plugs, Eastern Desert, Egypt. Bull NRC, Egypt, 26(3):303–319
Bozzola G, Dino GA, Fornaro M, Lorenzi A (2012) Technological innovations and new products obtained from a virtuos management of mining waste. In: Fourth international conference on engineering for waste and biomass valorisation, Porto, Portugal
Brown IWM, Mackenzie KJD (1992) Ceramic composites from waste glass. Ceramics 2:988–999
Brown TJ, Hobbs SF, Idoine NE, Mills AJ, Wrighton CE, Raycraft ER (2016a) European mineral statistics 2010–2014. British Geological Survey, Nottingham, p 378
Brown TJ, Idoine NE, Raycraft ER, Shaw RA, Deady EA, Hobbs SF, Bide T (2016b) World mineral production 2011–15. British Geological Survey, Nottingham, p 96
BS 1377 (1975) Moisture content and index tests, London, pp 50–100
Dondi M (1994) Compositional parameters to evaluate feldspathic fluxes for ceramic tile. Tile Brick Int 10(2):77–84
Dondi M (2018a) Feldspars and other fluxes for ceramic tiles: sources, processing, composition and technological behavior. Resour Conserv Recycl 133:191–205
Dondi M (2018b) Feldspathic fluxes for ceramics: sources, production trends and technological value. Resour Conserv Recycl 133:191–205
Dondi M, Guarini G, Venturi I (2001) Assessing the fusibility of feldspathic fluxes for ceramic tiles by hot stage microscope. Ind Ceramics 21(2):67–73
Dondi M, Raimondo M, Zanelli C (2014) Clays and bodies for ceramic tiles: reappraisal and technological classification. Appl Clay Sci 96:91–109
El-Maghraby MS, Ismail AIM, Belal ZL, Abd El-Shakour ZA (2019) Characterization and assessment of kaolinitic sand in ceramic industries. Interceram-Int Ceramic Rev 69:36–41
Espasito L, Tucci A, Naldi D (2005) The reliability of polishedporcelain stoneware tiles. J Eur Ceram Soc 25(9):1487–1498
Gharib ME, Obeid MA (2012) Paleozoic alkaline volcanism: geochemistry and petrogenesis of Um Khors and Um Shaghir trachytes of the central Eastern Desert Egypt. Arab J Geosci 5:53–71
Harris NBW (1982) The petrogenesis of alkaline intrusives from Arabia and northeast Africa and their implications for within plate magmatism. Tectonophysics 83:243–258
Hashad MH (1994) Geochemical characterization and petrogenesis of phonolite-trachyte plugs associated with Wadi Natash volcanic rocks. Middle East Res Centre Ain Shams Univ Earth Sci Ser 8:131–145
Jones JT, Berard MF (1972) Ceramics industrial processing and testing. Iowa state University Press, Ames
Kara A, Özer F, Kayaci K, Özer P (2006) Development of a multipurpose tile body: phase and microstructural development. J Eur Ceram Soc 26:3769–3782
Kayacı K (2021) The use of perlite as flux in the production of porcelain stoneware tiles. Bol Soc Esp Ceram Vidr 60(5):283–290
Klein G (2001) Application of feldspar raw materials in the silicate ceramic industry. Int Cer 50:8–11
Manfredini T, Pellacini GC, Romagloni M (1995) Porcelainized stoneware tiles. Am Ceram Soc Bull 74:76–79
Mohamed FH (2001) The Natash alkaline volcanic field, Egypt: geochemical and mineralogical inferences on the evolution of a basalt to rhyolite eruptive suite. J Volcanol Geotherm Res 105:291–322
Njoyaa FS, Tadjuidjea EJA, Ndzanaa A, Pountouonchia N, Tessier-Doyenb G (2017) Effect of flux content and heating rate on the microstructure and technological properties of Mayouom (Western-Cameroon) kaolinite clay-based ceramics. J Asian Ceram Soc 5:422–426
Sanchez E (2003) Technical considerations on porcelain tile product and their manufacturing process, part I. Int Ceram Rev 52(1):6–16
Sanchez E, Sanz V, Canas E, Sales J, Kayacı K, Taskıran MU, Anıl ÜE, Türk S (2019) Revisiting pyroplastic deformation. Application for porcelain stoneware tile bodies. J Eur Ceram Soc 39:601–609
Shalaby BNA, El-Maghraby MS, Mashaly AO, Salem AKA (2017) Geochemical characterization of Trachytic Rocks at Gabal Abu Hibban, Central Eastern Desert, Egypt, and their suitability as a flux in ceramic industry. Res J Appl Sci 12(2):242–253
Shalaby BNA, Ismail AIM, El-Maghraby MS (2018) Technological properties of high alumina refractories with different phosphoric acid contents. Bull Natl Res Cent 42:1–7
Shalaby BNA, Ismail AIM, Salem AKA (2019) The chemistry of allanite–britholite single crystal in alkaline volcanic rocks from Gabal Umm Shaghir area, central eastern desert, Egypt. SILICON 11:1809–1816
Stern RJ (1981) Petrogenesis, tectonic setting of late Precambrian ensimatic volcanic rocks, central Eastern desert of Egypt. Precam Res 16:195–230

Publisher's Note